Reduced-order molecular-dynamics model for polystyrene by equivalent-structure coarse graining

Anand Srivastava
Department of Mechanical Engineering, The Ohio State University, Columbus, Ohio 43210, USA

Somnath Ghosh*
Department of Civil and Mechanical Engineering, Johns Hopkins University, Baltimore, Maryland 21218, USA

(Received 4 October 2011; revised manuscript received 24 January 2012; published 13 February 2012)

This paper develops a reduced-order equivalent-structure based model for polystyrene in a rigid body molecular dynamics framework. In general, a coarse-grained model for polymers is obtained by replacing a group of chemically connected atoms by an effective particle and deriving a coarse-grained interaction potential that reproduces the structure and dynamics at the desired length and time scale. In the current model, a detailed (∼16 atoms) polystyrene monomer referred to as basic structural element (BSE) is replaced by an equivalent model with spherical backbone particles and an ellipsoidal particle that represents the styrene sidegroup. The governing principals of this homogenization is based on the mass, centroid, angular momentum, and energy equivalence between the detailed and the proposed reduced-order model. The bonded interactions parameters are readily obtained in the optimization of the equivalent structure from the detailed representation. The nonbonded interactions are treated separately. In order to capture the stereochemistry of the polystyrene molecule, an anisotropic biaxial nonbonded interaction potential function known as RE-squared (RE2) interaction has been used between pairs of ellipsoidal and/or spherical particles in the system. The required calibration of the nonbonded parameters is carried out by matching with the experimental density and the local structure using radial distribution function. This homogenization process scales up the modeling system size significantly as the higher frequency motions like -C-H- vibrations and sidegroup movements are suppressed. The accuracy of the model is established by comparing fine-scale simulation with explicit representations.

DOI: 10.1103/PhysRevE.85.026702 PACS number(s): 07.05.Tp, 83.10.Rs, 36.20.−r

I. INTRODUCTION

Molecular simulation methods, e.g., molecular dynamics (MD), have emerged as powerful techniques for studying static and dynamic properties of bulk amorphous polymers such as polystyrene or PS. Short-range structure and local heterogeneities at the nanometer scale can be evaluated in great detail using atomic trajectories that are generated from these simulations. The level of sophistication required for modeling polystyrene necessitates more than just linear chain models, because of the presence of phenyl groups at alternate backbone carbon atoms. This complex atomic structure poses severe computational challenges, especially when real polymeric systems are concerned. It is prohibitively demanding to solve real polymer physics problems using currently available computational resources. For example, in polymer thin-film experiments, the surface layer itself extends to as much as 10 nm [1]. An overall thickness of approximately 40 nm may provide adequate length scale effects in the simulation system to yield an acceptable degree of reliability in the molecular models [2]. In MD simulations, a 40-nm PS thin-film system would entail solving a system of equations for around 12 000 monomers. With periodic boundary conditions imposed on the 10 nm × 10 nm square region in the lateral plane along the *X*-*Y* directions, this is equivalent to solving for ∼200 000 atoms with explicit representation of hydrogen and carbon atoms or equivalently for ∼100 000 united atoms [3]. Coarse-grained or reduced-order representations of atomic systems are often implemented as a means of reducing computational requirements. In these models, explicit representation of every atom in the atomic system is replaced by "superatoms" that are units made up of a group of chemically connected atoms. Coarse graining also facilitates MD simulations on longer time scales that are typically necessary for simulating experimentally observed phenomena.

Generally speaking, the objective of coarse graining is to have as many atoms as possible in the reduced-order superatom unit to achieve maximum advantage in terms of computing at large length and time scales. However, coarse graining too many atoms into a single unit can result in a loss of local information like atomic packing and local arrangement. One of the widely practiced coarse-graining procedures was introduced by Tschöp and co-workers [4,5]. The underlying principle in this method is to identify the fast or high-frequency internal degrees of freedom from independent simulations of explicit isolated chains, and subsequent averaging. A number of other similar coarse-graining schemes have been proposed for polycarbonate and polystyrene systems in Refs. [6–8]. In particular, a variety of reduced-order models have focused on polystyrene [8–12], it being one of the most widely studied polymers with ample opportunity for experimental validation. The models are generally founded upon statistics-based potential of mean force inversion methodology, where interactions are obtained from sampling distributions using explicit atomistic simulation of isolated polymers. Since the sampling distribution functions are temperature dependent, the transferability of these models across a range of temperatures is subject to corrections. Besides temperature dependence, atomistic details like information on stereochemistry and

*Corresponding author: sghosh20@jhu.edu

sidegroup orientation are usually lost with coarse graining of the polymer structure. For example, such losses are evident in the 2:1 coarse-grained model for PS in Refs. [7,8,10], where each PS monomer is described by two coarse-grained (CG) superatoms. The superatoms in this model are spherical in nature with the sidegroup compressed in the backbone. To improve the stereochemistry representation, some models have made special provisions to account for the different tacticities of adjacent monomers [9]. Different potential functions are defined based on the whether the initial state of monomer pairs was racemic or meso in nature, thus making the method dependent on initial structure. Moreover, since the coarse-grained particle is generally assumed to be spherical, anisotropic phenomena like alignment of polystyrene sidegroups in the direction of applied strain [13] cannot be captured using these models.

The proposed coarse-grained model in this study is developed to overcome some of the shortcomings mentioned above. In this model, a monomer is replaced by an equivalent structural element, where the sidegroup is configurationally represented as an ellipsoid. The three backbone united atoms make up the other units of the basic structural element of the molecular chain structure. To overcome the limitations of orientation dependence associated with conventional coarse-graining methods, a rotational dynamics based MD framework is implemented in the software LAMMPS [14]. The reduced-order model is capable of reproducing the basic structural properties like density and pair-correlation function of the explicit MD model. It is expected that it will enable larger polymeric nanosystems (∼40–100 nm) to be studied within the constraints of available computational resources.

II. REPRESENTATION OF AN EQUIVALENT BASIC STRUCTURAL ELEMENT

Figure 1(a) shows an atomic scale representative volume element (RVE) for PS with explicit representation of molecular chains and configurations. The corresponding basic structural element (BSE) delineating the fundamental constitution of the material at this scale is shown in Fig. 1(b). Coarse graining to generate reduced-order MD models of PS is executed in two stages. In the first stage, the BSE that corresponds to an explicit PS monomer consisting of ∼16 atoms is reduced to a united atom representation as shown in Fig. 2(a). In this nominally reduced-order representation, the chemically connected hydrogen and carbon atoms are consolidated into one united atom that is assumed to be a spherical point with zero volume or no moment of inertia. Subsequently, each monomer consists of nine united atoms as shown in Fig. 2(a). Detailed studies of PS with this united atom representation have been carried out by the authors in Refs. [3,15]. In the second stage of coarse graining, the phenyl ring of PS monomer is replaced by an equivalent ellipsoid, and consequently the BSE consists of four structural units as shown in Fig. 2(b). The three backbone united atoms are represented as spherical particles, whereas the phenyl sidegroup is represented as a single ellipsoidal rigid body. The repeat unit of the BSE is shown in Fig. 2(b), where backbone atoms are labeled A and B, while the phenyl sidegroup is labeled C.

The configuration and geometric properties of the ellipsoid are determined from its structural equivalence with the explicit system, i.e., by equating the zeroth-, first-, and second-order moments of inertia of the ellipsoid with those of the sidegroup atoms in the BSE. As shown in Fig. 2(c), the phenyl sidegroup in the PS monomer consists of six united atoms in the explicit styrene ring. Equating the zeroth moment of inertia conserves the total mass of the system and determines the volume of the equivalent ellipsoid. Thus

$$m^{\text{ell}} = \sum_{i=1}^{6} m_i, \tag{1}$$

where m^{ell} is the total mass of the equivalent ellipsoid and m_i is the mass of individual particles in the united atom representation. The six atoms are labeled C_3 to C_8 in Fig. 2(a) with masses of 12 atomic mass units or amu for C_3 and 13 amu for the other five resulting in a total ellipsoid mass of 77 amu.

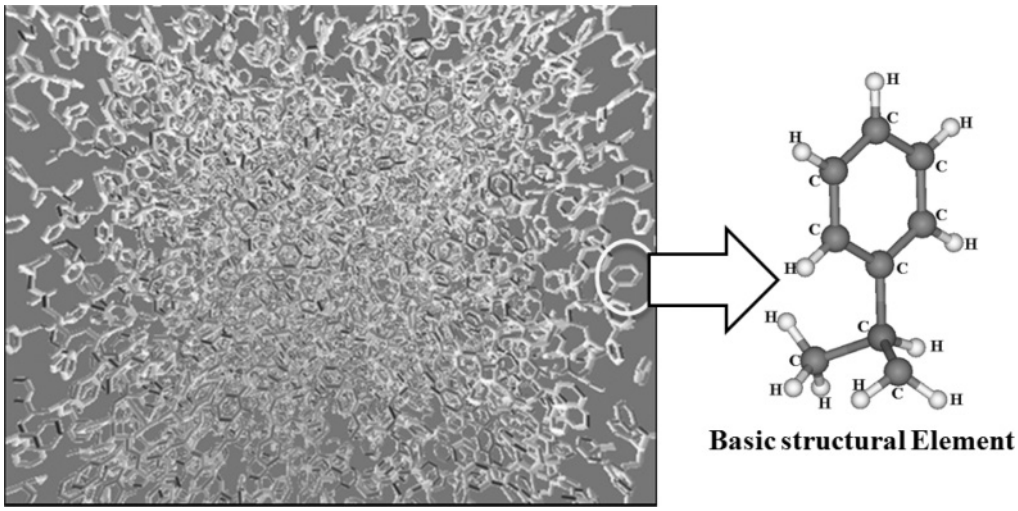

FIG. 1. (a) Representative volume element (RVE) of a polystyrene system, and (b) the basic structural element (BSE) representing the fundamental building block of the molecular chain.

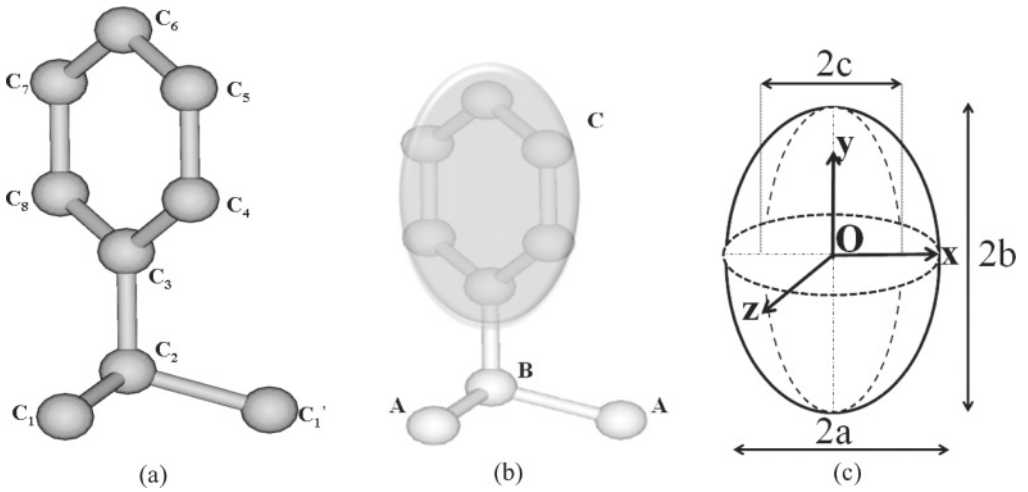

FIG. 2. (a) Stage 1 reduced order: united atom representation; (b) stage 2 reduced order: equivalent ellipsoidal representation; (c) sidegroup as ellipsoid with axial lengths.

The bond length between the chemically connected atoms is ∼1.4 Å.

Equating the first moment of inertia conserves linear momentum and determines the centroid position of the ellipsoid. The centroidal coordinates x_c^{ell}, y_c^{ell}, and z_c^{ell} of the equivalent ellipsoid are thus expressed as

$$x_c^{\text{ell}} = \frac{\sum_{i=1}^{6} m_i x_i}{\sum_{i=1}^{6} m_i}, \quad y_c^{\text{ell}} = \frac{\sum_{i=1}^{6} m_i y_i}{\sum_{i=1}^{6} m_i}, \quad z_c^{\text{ell}} = \frac{\sum_{i=1}^{6} m_i z_i}{\sum_{i=1}^{6} m_i}, \tag{2}$$

where x_i, y_i, and z_i are the position coordinates of the ith united atom in the phenyl sidegroup.

Finally, equating the second moments conserves angular momentum and determines the principal axes directions. The second moment of inertia for the phenyl group of six atoms is defined as

$$\mathbf{I} = \sum_{i=1}^{6} m_i(\mathbf{r}_i \otimes \mathbf{r}_i), \tag{3}$$

where m_i and $\mathbf{r_i}$ are mass and position vector of the six particles in the united atom representation, respectively, and $\otimes$ is the tensor product symbol. While mass and centroid are uniquely determined for the ellipsoid, the nine moments of inertia for the three principal axes and the corresponding three principal directions gives rise to an overdetermined system of equations. Consequently, a minimization scheme is employed to obtain the best fitting second moment of $\mathbf{I}$ for the equivalent ellipsoid from a hexagonal arrangement of atoms. The three eigenvalues of the second moment of inertia I_1, I_2, and I_3 provide the three principal axis lengths ($2a$, $2b$, and $2c$) of the equivalent ellipsoid, from the following equations:

$$a = \sqrt{\frac{5(-I_1 + I_2 + I_3)}{2m^{\text{ell}}}}, \quad b = \sqrt{\frac{5(I_1 - I_2 + I_3)}{2m^{\text{ell}}}}, \quad c = \sqrt{\frac{5(I_1 + I_2 - I_3)}{2m^{\text{ell}}}}. \tag{4}$$

For the polystyrene phenyl ring, the principal axes lengths a, b, and c of the equivalent ellipsoid are found to have values of 3.45 Å, 3.45 Å, and 1.0 Å, respectively. This corresponds to a spheroid.

The orientations of the three principal axes $\mathbf{x}'$, $\mathbf{y}'$, and $\mathbf{z}'$ can be determined as the eigen-vectors of the second moment of inertia matrix $\mathbf{I}$. Various types of orientation representation include the rotation matrix, axis angles, or Euler angles. Alternatively, a singularity free, four parameter quaternion representation, introduced in Ref. [16], is implemented for designating orientation. Unlike Euler angles, quaternions do not suffer from the possibility of "gimbal lock," when two planes overlap causing one of the Euler angles to become ambiguous. Quaternion algebra is numerically more stable and requires far less number of parameters to be stored than in the rotation matrix representation. Like real number and complex number systems, quaternions correspond to a number system that can be used to represent a point in space by a single number or quaternions [17].

The quaternion rotation is written as a normalized four-dimensional vector,

$$\hat{\mathbf{q}} = [q_0\ q_1 i\ q_2 j\ q_3 k]^{\top}, \tag{5}$$

where $q_1^2 + q_2^2 + q_3^2 + q_4^2 = 1$. Furthermore, according to the quaternion number system mathematics [16], $i^2 = j^2 = k^2 = ijk = -1$. Calculating the quaternion of a given phenyl sidegroup in the reduced-order system involves the derivation of a orientation matrix $\mathbf{Q}$ for the BSE and calculation of its eigenvalues and eigenvectors.

The process is first executed on the staring configuration to generate the initial configuration of the reduced-order system. The centroidal position and quaternions of the reduced-order system evolve with subsequent increments of the molecular-dynamics simulations. The orientation matrix for the ellipsoid is written in terms of three orthogonal basis vectors, derived for the phenyl sidegroup. The $\mathbf{x}'$ direction is in the plane perpendicular to the phenyl ring, while the line joining atoms C_3 and C_6 in Fig. 2(a) is assumed to correspond to the $\mathbf{z}'$

TABLE I. Degrees of freedom (DOF) associated with different stages of reduced-order representation of polystyrene in MD simulations.

Units or DOF	Explicit atom system	United atom system	Equivalent ellipsoid system
No. of units or monomer	16	9	4
DOF or monomer	48	24	13
DOF (1 × 80 monomers)	∼3840	∼1920	∼1040
DOF (8 × 320 monomers)	∼122880	∼61440	∼33280

direction. The $\mathbf{y}'$ direction is constructed from the line joining the bisectors of the lines C_4-C_5 and C_7-C_8, respectively,

$$\mathbf{Q} = \begin{bmatrix} x'_1 & y'_1 & z'_1 \\ x'_2 & y'_2 & z'_2 \\ x'_3 & y'_3 & z'_3 \end{bmatrix}. \tag{6}$$

The eigenvalues of $\mathbf{Q}$ are given as

$$\lambda = \{1,\ \cos(\theta) + i\ \sin(\theta),\ \cos(\theta) - i\ \sin(\theta)\}, \tag{7}$$

where θ is the rotation angle. The eigenvector ($\hat{\mathbf{e}}$) corresponding to eigenvalue 1 is an invariant principal axis of rotation. The four components of quaternions are expressed in terms of the principal axis $\hat{\mathbf{e}} = [e_1\ e_2\ e_3]^\top$ and the angle θ as

$$\begin{aligned} q_0 &= \cos(\theta/2), \quad q_1 = e_1 \sin(\theta/2), \\ q_2 &= e_2 \sin(\theta/2), \quad q_3 = e_3 \sin(\theta/2). \end{aligned} \tag{8}$$

At any given instance, quaternions can also be used to obtain the rotation matrix as

$$\mathbf{R} = \begin{bmatrix} -1 + 2q_1^2 + 2q_0^2 & 2(q_1q_2 - q_3q_0) & 2(q_1q_3 + q_2q_0) \\ 2(q_1q_2 + q_3q_0) & -1 + 2q_2^2 + 2q_0^2 & 2(q_2q_3 - q_1q_0) \\ 2(q_1q_3 - q_2q_0) & 2(q_1q_0 + q_2q_3) & -1 + 2q_3^2 + 2q_0^2 \end{bmatrix}. \tag{9}$$

The mass, centroidal position, orientation in terms of quaternions, and the principal axes lengths complete the description of the equivalent ellipsoidal rigid-body sidegroup of the PS monomer at any time instance. The other three particles that form the backbone are simply represented by their position vectors with no size (hence zero moment of inertia). Their quaternion parameters $[q_0 q_1 q_2 q_3]$ stay constant at [1 0 0 0]. Table I depicts the system size and total degree of freedoms for a system with eight chains and 320 monomers corresponding to different stages of coarse graining.

The reduced-order system decreases the degrees of freedom by approximately a factor of 3.6 for the eight chain, 320 monomer model.

III. POTENTIAL-ENERGY FUNCTIONS OF THE REDUCED-ORDER SYSTEM

Atoms in the polymeric chains are chemically connected by various springs and joints that provide the bonded interactions and maintain the kinematics and the local morphology of the polymer chain. Besides the bonded interactions, the dynamics of atoms in the polymer chains are also governed by nonbonded interactions. These are nonlocal in nature and take place between atoms, which are not bonded directly. Thus the molecular interactions for a polymer system includes bonded energy (U_{bd}) and nonbonded energy (U_{nb}) terms. The total potential energy (U_{total}) of the system is thus written as (see [15])

$$U_{\text{total}} = U_{\text{bd}} + U_{\text{nb}}. \tag{10}$$

The bonded and nonbonded interactions for the reduced-order model are discussed next.

A. Bonded interactions

The configuration and kinematics in the explicit representation of polymeric chains are effectively modeled by including terms like angular, torsional, improper, and out-of-plane interactions along with the springlike bond interactions as shown in Fig. 3. The potential function in the explicit model for bonded interaction is given as [3,15]

$$\begin{aligned} U_{\text{bd}} = {} & \frac{1}{2}k_b(r - r_0)^2 + \frac{1}{2}k_\theta(\theta - \theta_0)^2 + \frac{1}{2}\sum_{j=1}^{3} k_\phi^j \\ & \times [1 + (-1)^{j+1}\cos j(\phi)] + \frac{1}{2}k_\psi(\psi - \psi_0)^2. \end{aligned} \tag{11}$$

Here r_o, θ_o, and ψ_o are the equilibrium bond length, angle, dihedral angle, and improper angle, respectively, and k_b, k_θ, k_ϕ, and k_ψ are the corresponding stiffness coefficients.

Development of the functional form for the bonded potential of the reduced-order model is executed in the following steps.

(1) MD simulation of the full monomer chain system in its explicit representation is carried out at a given temperature.

(2) The centroidal positions of random particle pairs A and B [see Fig. 2(b)] in the ensemble are determined and their trajectory is sampled for distribution of bond lengths AB,BC, angles ABA and ABC, and dihedral angle ABA′B′. This sampling is done for approximately 1000 temporal instances so

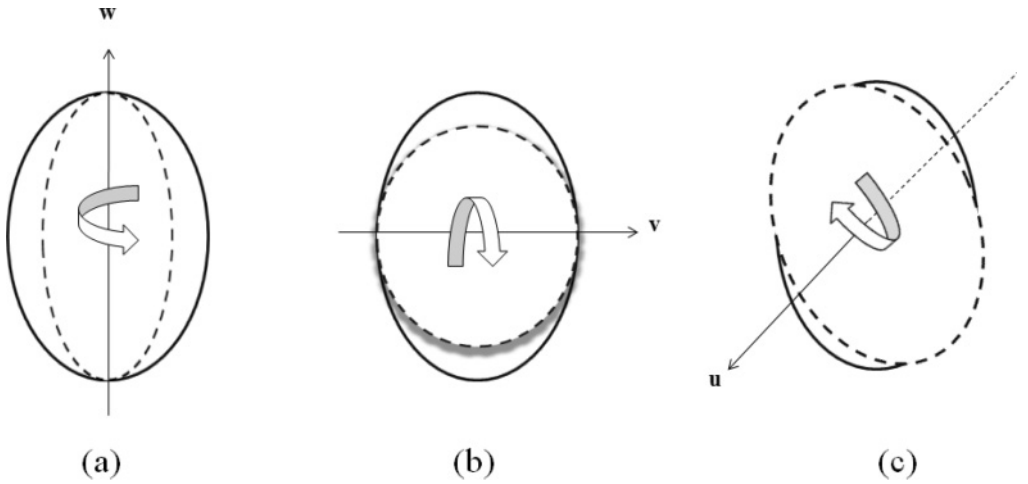

FIG. 3. Modes of deformation: (a) twisting; (b) out-of-plane bending; (c) in-plane deformation.

that a reliable statistics can be developed for the reduced-order model.

(3) Distribution functions $P(r)$, $P(\theta)$, and $P(\phi)$ for the chains are obtained from the above sampling. A rigorous convergence study is carried out to ensure that these probability distributions are statistically unbiased and independent of the number of sampling points.

(4) These probability distributions correspond to the Boltzmann factors of the generalized intrachain interaction potentials $U(r)$. These are written as

$$P(r) = \exp\left\{\frac{-U(r)}{k_B T}\right\}, \tag{12}$$

$$P(\theta) = \exp\left\{\frac{-U(\theta)}{k_B T}\right\}, \tag{13}$$

$$P(\phi) = \exp\left\{\frac{-U(\phi)}{k_B T}\right\}, \tag{14}$$

where k_B is the Boltzmann's constant, $U(r)$ is the bonded-length potential of the reduced-order chain model, and $U(\theta)$ and $U(\phi)$ are the corresponding bond angle and torsion potentials. Thus far there is no fitting procedure needed and it is directly the result of mapping energetic and entropic contributions from the finer scale explicit model.

(5) As an example, the coefficient for the assumed bond-stretching potential function of the reduced-order model is obtained directly from Eq. (14) as

$$U(r) = -k_B T \ln P(r) + C_r. \tag{15}$$

The coefficient C_r is added and evaluated to keep the minimum bond-length potential to zero. Consequently, its value is $C_r = k_B T \ln P(r_0)$. The bond-stretching potential for the reduced-order model is assumed to be harmonic. Correspondingly, the coefficient K_r is obtained from the equation

$$U_r = \frac{K_r}{2}(r - r_0)^2 = -k_B T \ln P(r) + C_r. \tag{16}$$

The same procedure is repeated for the other bonded potential functions as well. (See Fig. 4.)

For bonded interactions, the functional form of bond angle bending modes is described using an harmonic potential, expressed as

$$U_{\text{angle}} = \frac{K_\theta}{2}(\theta_k - \theta_0)^2. \tag{17}$$

Values for the constants K_r, r_0, K_θ, and θ_0 are listed in Table II.

The functional form for the torsional interaction is chosen to describe rotation along the bonds in the backbone carbon atoms in accordance with the transferable potentials for phase equilibria (TraPPE) potential form [3]:

$$U_{\text{torsion}} = \tfrac{1}{2}\{k_\phi^1[1 + \cos(\phi)] + k_\phi^2[1 - \cos(2\phi)] + k_\phi^3[1 + \cos(3\phi)]\}. \tag{18}$$

Again the values of the constants are listed in Table II. One of the consequences of coarse graining is the possibility of loss of configurational integrity due to removal of hydrogen atoms

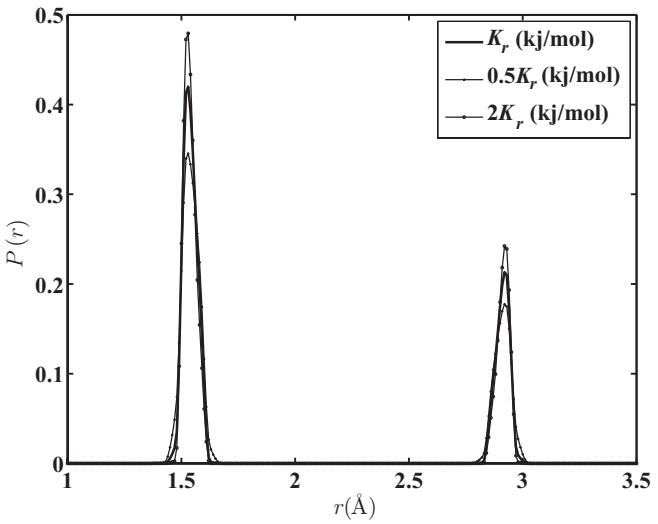

FIG. 4. Probability distribution with respect to bond length. A higher K_r has sharper and higher peak and narrower spread than a lower K_r. The figure shows distribution for original stiffness value as well as distribution when the stiffness is halved and doubled.

TABLE II. Potential function parameters for reduced-order representation of the polystyrene system. Different units of angles for equilibrium values (degree) and force constants (radians) are used in the table to maintain consistency with the representation followed in the molecular-dynamics software package LAMMPS that was used to carry out the simulations.

Chemical bonds	(kj/mol/Å^2)	r_0 (Å)
A-B	666.00	1.54
B-C	1000.00	2.91
Angular bonds	k_θ (kJ/mol/rad^2)	θ_0 (deg)
A-B-A′	520.0	112.0
A-B-C	1000.0	120.0
Dihedral bonds	k_ϕ^1 (kJ/mol) k_ϕ^2 (kJ/mol)	k_ϕ^3 (kJ/mol)
A-B-A′-B′	5.904 −1.124	13.158
Improper bonds	k_ψ (kJ/mol/rad^2)	ψ_0 (deg)
B-C-A-A′	167.40	31.00

at the chiral centers. As a result, the four united atoms, C_1, C_2, C_3, and $C_1^{'}$ tend to collapse into one plane. In order to prevent this collapse, an improper dihedral-angle interaction potential has been proposed in Refs. [8,18] as

$$U_{\rm imp} = \frac{K_\psi}{2}(\psi_k - \psi_0)^2, \tag{19}$$

where ψ is the improper dihedral angle that conserves the structure of the chiral center in the molecules modeled as united atoms. The corresponding forces cause the unit normal to the plane (C_1,C_2,C_3) to oscillate about its mean position. To coincide with the equilibrium position obtained from MD simulations with explicit structure representation, an equilibrium value $\psi_0 = 35.04^\circ$ is used with the united atom potential. This is the angle formed with the -C_2-H- vector in the equilibrium position. Though $\psi_0 = 35.04^\circ$ was used for the united atom simulation, the mean value of probability distribution for the equivalent angle in the new representation of C, A, B, A′ was found to be 31°. One possible reason for this deviation may be the difference in coordinates of site C_3 in united atom representation and site C in equivalent coarse-grained representation.

B. Nonbonded interactions for rigid-body systems

Normally, nonbonded interactions between individual atoms are represented in terms of distance-dependent potential functions. An example is the Lennard-Jones (LJ) potentials, where particles are assumed to be spherical and interactions have radial symmetry. However, approximating a group of atoms as a spherical particle has its shortcomings, especially for systems like the phenyl sidegroup, where the six atoms are arranged as part of a coplanar hexagon. If the physical properties are dependent on the stacking direction of the sidegroup, the spherical assumption may be misleading. In Ref. [13], it has been shown that phenyl sidegroups in polystyrene chains tend to align themselves in the direction of applied tension when a uniaxial load is applied. If the sidegroup is assumed to be spherical, this alignment cannot be captured when the system is subjected to an external load. In order to retain the anisotropy in a reduced-order model framework, the sidegroups are assumed to form a rigid body with moments of inertia specified from the explicit atomic structure.

In this work, the styrene sidegroup is represented as a spheroidal rigid body, based on the geometry of the phenyl ring as discussed in Sec. II. Gay-Berne [19] have introduced the *ellipsoidal* potential as an extension of LJ potential for anisotropic particles. Parameters of the Gay-Berne potential, however, lack a well-defined physical interpretation and their calibration can be erroneous. A modification to Gay-Berne potential was proposed in Ref. [20], where the parameters are related to the equilibrium energy, distance, and orientation in a more physical way. This potential is termed the RE-squared (RE2) potential. The potential energy $V_{\rm RE2}$ is broken down into an attractive $V_{\rm RE2}^A$ and a repulsive interaction energy part $V_{\rm RE2}^R$ and is expressed as

$$V_{\rm RE2}(\mathbf{r}_1,\mathbf{q}_1,\mathbf{r}_2,\mathbf{q}_2) = V_{\rm RE2}^A(\mathbf{Q}_1,\mathbf{Q}_2,\mathbf{r}_{12}) + V_{\rm RE2}^R(\mathbf{Q}_1,\mathbf{Q}_2,\mathbf{r}_{12}), \tag{20}$$

where $\mathbf{Q}_1$ and $\mathbf{Q}_2$ are the transformation matrices from the global reference frame to the local frame and $\mathbf{r}_{12}$ is the position vector joining the centroid of the particles. Since the rotational degrees of freedom are also included in this potential function via $\mathbf{Q}_1$ and $\mathbf{Q}_2$, RE2 functional form is able to capture and evolve the different modes of deformation for the phenyl group as shown in Fig. 3. As a result, the modes of deformation like twisting, in-plane, and out-of-plane motion of the phenyl group are simulated without explicitly using any bonded potential like torsional spring potentials. Moreover, the selection of parameters with the RE2 form are very physical in nature. The RE2 form gives the approximate interaction energies between ellipsoids and spheres instead of a modified LJ-based formulation as in the Gay-Berne potential [21]. RE2 potential is formulated in a way that the orientation dependence decays at large distances and asymptotically reduces to the interaction energy between two spheres. Moreover, it is known to give a more realistic intermediate and close contact interaction [20]. The full details of RE2 formulation can be obtained from [20,22].

C. Numerical values of the nonbonded parameters

From a purely computational viewpoint, the RE2 potential interaction between particles in the system can be defined if diagonal shape tensor $\mathbf{S}_i$ and the relative well-depth values along with the Hamaker constant A12 and the atomic interaction radius σ are known. The shape tensor $\mathbf{S}_i$ ($i = 1,2$) is given in terms of the three principal radii a_i, b_i, and c_i of the ellipsoid as

$$S_i = \begin{pmatrix} a_i & 0 & 0 \\ 0 & b_i & 0 \\ 0 & 0 & c_i \end{pmatrix}. \tag{21}$$

The relative well depth for each site can be expressed as

$$\epsilon_x = \sigma\frac{a}{bc}, \quad \epsilon_y = \sigma\frac{b}{ac}, \quad \epsilon_z = \sigma\frac{c}{ab}. \tag{22}$$

TABLE III. RE2 parameters for the reduced-order model.

Particle	A-A	B-B	C-C	A-B	A-C	B-C
σ	3.95	4.65	5.00	4.30	4.48	4.83
ϵ_x	3.95	4.65	5.00	4.28	4.44	4.82
ϵ_y	3.95	4.65	5.00	4.28	4.44	4.82
ϵ_z	0.3318	0.3906	0.42	0.36	0.3733	0.4050
A_{12}	30.24	32.22	86.24	30.22	50.61	50.61
σ_c	10.00	10.00	12.00	10.00	12.00	12.00

To define nonbonded interactions between ellipsoidal and/or spherical particles using RE2 anisotropic potential in LAMMPS [14], the following parameters must be exactly defined for each pair of atoms: $A12_{ij}$ = Hamker constant or energy prefactor for the pair (kj/mol); σ_{ij} = radius of the particle that represents excluded volume for the pair (Å); ϵ_{xi} = relative well depth of particle i for side-to-side interactions; ϵ_{y_i} = relative well depth of particle i for face-to-face interactions; ϵ_{z_i} = relative well depth of particle i for end-to-end interactions; ϵ_{xj} = relative well depth of particle j for side-to-side interactions; ϵ_{y_j} = relative well depth of particle j for face-to-face interactions; ϵ_{z_j} = relative well depth of particle j for end-to-end interactions; σ_c = cutoff distance (Å).

The face of the side-group is in the plane of the phenyl ring. The end-to-end is the normal to the plane of the ring. These are easily obtainable geometric properties of the ellipsoids and spherical sites for the molecule under investigation. The simplification in terms of parametrization is made by using the assumption from Derjaguin expansion [23], where energy well depth parameters are expressed in terms of local curvatures of the ellipsoid.

The three kinds of particles used in the coarse graining are denoted by A, B, and C, where A and B are the spherical backbone atoms and C is the ellipsoidal sidegroup. The calibrated parameters for nonbonded interactions used in this work are presented in Table III. A series of calibration simulations were run with the chosen parameters before arriving at the final values. Tests were performed to observe energy conservation and these simulations were validated against radius of gyration, radial distribution function, and the density of the PS system. The final interaction radius σ for spherical sites is chosen to be 3.95 Å and 4.65 Å, respectively. These values are the same as the interaction radius used in the united atom representation [3,8]. A larger value of 5.0 Å was chosen for the interaction radius of the ellipsoidal site C. An arithmetic mean is used to obtain interaction values for unlike pairs of particles. The values for relative well depth are obtained using Eq. (22) for each pair. Geometric mean is used to obtain the relative well depth for unlike sites. The cutoff distance σ_c was chosen to be equal to the united atom cutoff distance of 10 Å for particles A and B. A value of 12 Å was used for ellipsoidal particle C, since it has bigger dimension and longer range for nonbonded interactions. The initial values of prefactor A12 of the potential energy term (Hamaker constants) were guessed to be 30 kj/mol for spherical sites and 80 kj/mol for the ellipsoidal sites and were optimized by matching the total potential energy of the CG system with the energy from the united atom simulation. The final values are shown in Table III.

IV. SIMULATION RESULTS AND VALIDATION

Three PS systems containing different numbers of chains and monomers are studied in this work for coarse graining. They are (1) a system containing one chain of 80 monomers, (2) a system containing one chain of 320 monomers, and (3) a system consisting of eight chains of 320 monomers.

The initial configuration of each system is obtained from a fully equilibrated explicit MD system. As discussed in Refs. [3,15], PS molecules in the explicit model are assembled using the augmented phantom chain growth or PCG scheme. In this algorithm, monomers are introduced based on a sampling of a uniform random distribution of the backbone dihedral angle. The total energy change ΔU resulting from the introduction of a new site is calculated as the sum of the dihedral and nonbonded interactions. The probability of the acceptance of the new monomer is given by

$$p = \min[1, \exp(-\beta \Delta U)], \tag{23}$$

where β is the product of Boltzmann constant k_B and the temperature of the system. If a new monomer is not accepted after a certain number of trials, the chain is shortened by removing the previous monomer, and the procedure is repeated.

The initial coordinates and the orientation of the ellipsoids are obtained using methods discussed in Sec. II. The initial velocity and angular velocity of the ellipsoids are assigned randomly such that total momentum is zero and the total kinetic energy is proportional to the desired temperature. The system is validated at 350 K. A time step of 4 fs is chosen for this work and the simulation at each temperature is run for approximately 2 ns. The reduced-order model is tested by mapping the coarse-grained trajectory at the end of the simulation to a full scale local structure to confirm if the atomic level topology is retained. Also, the robustness of the potential function developed for the reduced-order model is tested through convergence of radial distribution functions and density at a temperature 350 K. The simulated densities at different temperatures are found to be within a 10% error range.

Figure 5 exhibits the result of reinsertion of atomic details in the molecular model at the end of the simulation. A 3 monomer strip from the chain of 320 monomers is chosen to highlight the remapping of the reduced-order system to the detailed atomic system. Figure 5(a) corresponds to the coarse-grained data obtained from MD simulation at a given time step. Figure 5(b) shows the 3 monomer system after it has been reconstructed using the information about coordinates and orientation embedded in the reduced-order model trajectory. The backbone atoms are trivially mapped as they represent coordinate positions of the same particles in both reduced-order and united atom manifestations. The large ellipsoidal particle in the reduced-order system contains in itself the evolved centroid and orientation information. Due to this information, the ellipsoid can be mapped back accurately to the corresponding styrene sidegroup as shown in the figure. The mathematical details of this exercise are detailed in

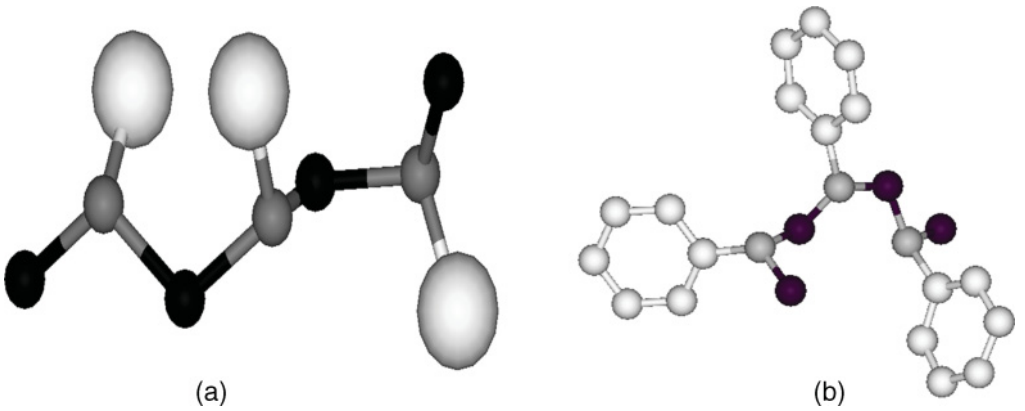

FIG. 5. (Color online) (a) Three monomer sample in the reduced-order representation; (b) the reconstructed united atom system at the end of the simulation.

Sec. II. The above result shows that, besides retaining the information about the centroid position of the CG site like other sphere-based models [7–11], the current model also evolves the orientational degree of freedom because of its anisotropic nature. Consequently, a finer all-atom or united atom system can be easily and accurately obtained from the existing coarse-grained system if required.

The radial distribution function for a reduced-order ellipsoid-ellipsoid system is plotted in Fig. 6. As demonstrated in the figure, there is a local peak due to near-neighbor correlation, which decays to unity after a length of 10 Å. This behavior is consistent with the theory. It also validates the local structural inhomogeneity and far-field homogenized behavior. Figure 7 shows the density convergence of the reduced-order system at 350 K. The density converges to experimental values within an error of 10%. This is acceptable for this significant level of coarse graining. Furthermore, the rate of convergence of the reduced-order model is much faster than what is observed in full scale MD simulation [3], thus establishing the advantage of this model.

One of the primary objectives of this coarse graining is to facilitate and expedite the process of estimating the glass transition temperature T_g of bulk and thin-film polystyrene systems. For numerical evaluation, the simulation is executed for a temperature range from 300 to 450 K in 25 K intervals under a constant pressure state. Periodic boundary conditions are applied to the reduced-order simulation boxes. The simulation is run for about 2 ns at each temperature until convergence in density is achieved. The densities are plotted as a function temperature in Fig. 8. The simulation results are within a range of 10% of the experimental value reported in Ref. [24] as 370 K. The glass transition is underpredicted by about 15 to 20 K using this method. However, given the scale of coarse graining involved and the model's ability to accurately capture the molecular-level anisotropy, the T_g value is believed to be predicted within an acceptable range. The difference with experimental value can be attributed to a variety of different factors, such as cooling rate and sampling limitations of MD, along with the parametrization done in this work. However, a reasonable estimate about the glassy phase transition in the polymeric system can be made within a

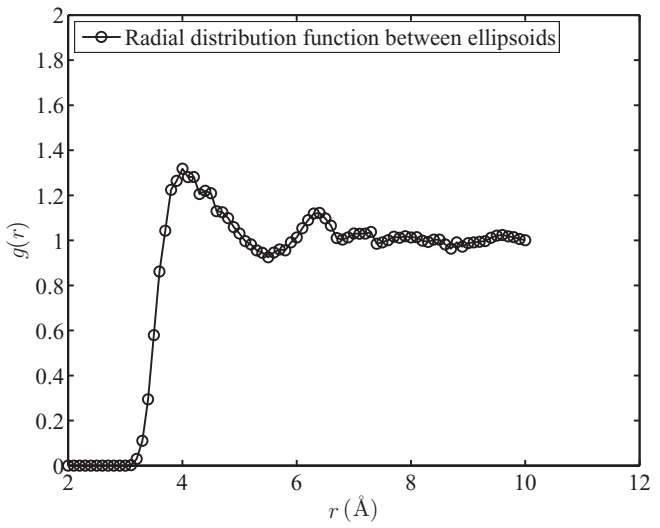

FIG. 6. Radial distribution function of ellipsoidal particle system.

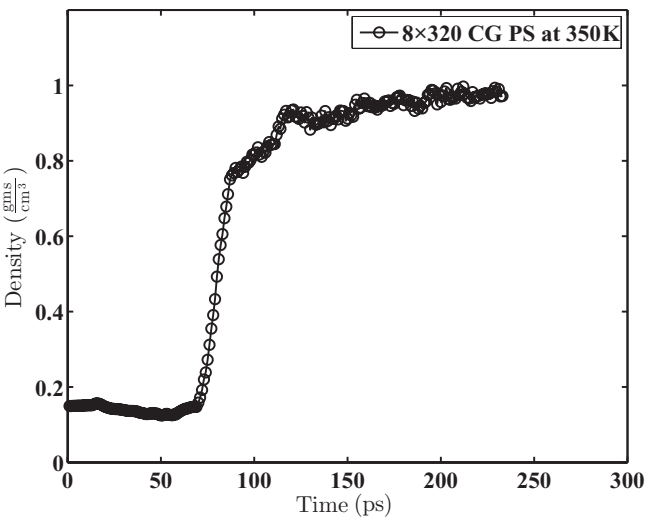

FIG. 7. Convergence in density at 350 K with the reduced-order model. The initial system has very sparse density (∼0.2 gcc) and the CG model shows a very fast convergence to the experimental scale density. The experimental density of PS is ∼1.05 gcc at room temperature.

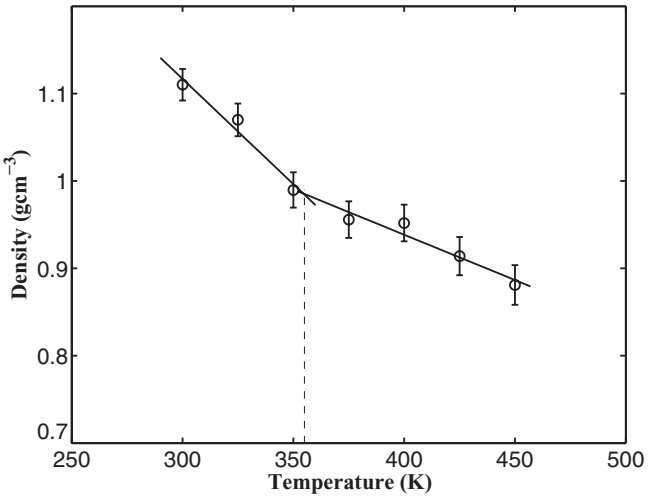

FIG. 8. Density of PS between 300 and 450 K with the reduced-order model. The bold lines are least square fit to the density data. The dashed vertical line is drawn to locate the point of intersection of the two fitted lines, originating from the two ends. Temperature value at the intersection is found to be 355 K. This is taken as the simulation T_g value, estimated at the temperature where the coefficient of thermal expansion changes. The experimental value of T_g is ∼370 K.

range, based on the density plots, using the current method. Tranferability of simulation parameters across temperatures is a known limitation in the coarse-graining literature [12], which makes any prediction pertaining to T_g debatable. As shown in Fig. 8, the slope of the curve signifying the coefficient of thermal expansion is observed to change at around ∼350 K. This temperature can be assumed to signal the onset of the glassy phase and is an estimate of T_g.

V. CONCLUSION

A molecular structurally equivalent reduced-order model is developed for polymers in this work. The overall intent of this coarse graining is to bridge the gap in length and time scales between experiments and computational models such that longer time periods may be simulated. A statistically equivalent, reduced-order model for polystyrene is arrived at by rigorous sampling of the fine-scale trajectory. The model is shown to reproduce basic structural properties like density and pair-correlation function within acceptable tolerances. While this coarse-graining method has been applied to the polystyrene system only in the current work, the model can be used to study realistic nanosystems (∼40–100 nm) of polymeric materials within the available computational resources.

ACKNOWLEDGMENTS

This work has been supported by the NSF Division of Engineering Education & Centers through Grant No. EEC-0425626 to the Center for Affordable Nanoengineering of Polymeric Biomedical Devices (CANPBD) at the Ohio State University. This sponsorship is gratefully acknowledged. Computer support by the Ohio Supercomputer Center through Grant No. PAS813-2 is also gratefully acknowledged.

[1] J. A. Forrest, Eur. Phys. J. E **8**, 261 (2002).
[2] C. Alleman, A. Srivastava, and S. Ghosh, J. Polym. Sci., Polym. Phys. **49**, 1131 (2011).
[3] A. Srivastava and S. Ghosh, Int. J. Multiscale Comp. Eng. **8**, 535 (2010).
[4] W. Tschöp, K. Kremer, J. Batoulis, T. Bürger, and O. Hahn, Acta Polym. **49**, 61 (1998).
[5] W. Tschöp, K. Kremer, O. Hahn, J. Batoulis, and T. Bürger, Acta Polym. **49**, 75 (1998).
[6] D. Reith, M. Pütz, and F. Müller-Plathe, J. Comput. Chem. **24**, 1624 (2003).
[7] R. Faller, Polymer **45**, 3869 (2004).
[8] V. A. Harmandaris, N. P. Adhikari, N. F. A. van der Vegt, and K. Kremer, Macromolecules **39**, 6708 (2006).
[9] G. Milano, S. Goudeau, and F. Müller-Plath, J. Polym. Sci. Part B, Special Issue on Multiscale Modeling of Polymers **43**, 871 (2005).
[10] Q. Sun and R. Faller, Comput. Chem. Eng. **29**, 2380 (2005).
[11] G. Santagelo, A. di Matteo, F. Müller-Plath, and G. Milano, J. Phys. Chem. B **111**, 2765 (2007).
[12] W. Mattice, Y. Tatek, and N. Waheed, Macromolecules **40**, 379 (2007).
[13] A. Lyulin, N. Balabaev, M. Mazo, and M. Michels, Macromolecules **37**, 8785 (2004).
[14] S. Plimpton, J. Comput. Phys. **117**, 1 (1995).
[15] A. Srivastava, C. Alleman, S. Ghosh, and L. J. Lee, Modell. Simul. Mater. Sci. Eng. **18**, 065003 (2010).
[16] H. Goldstein, *Classical Mechanics* (Addison-Wesley, Reading, MA, 1950).
[17] L. D. Landau and E. M. Lifshitz, *Mechanics* (Pergamon Press, New York, 1976).
[18] C. Wick, M. Martin, and J. I. Siepmann, J. Phys. Chem. B **104**, 8008 (2000).
[19] J. G. Gay and B. J. Berne, J. Chem. Phys. **74**, 3316 (1981).
[20] R. Everaers and M. R. Ejtehadi, Phys. Rev. E **67**, 041710 (2003).
[21] B. J. Berne and P. Pechukas, J. Chem. Phys. **56**, 4213 (1972).
[22] R. E. M. Babadi and M. R. Ejtehadi, J. Chem. Phys. **124**, 174708 (2006).
[23] B. V. Deryaguin, Kolloid Z. **69**, 155 (1934).
[24] T. Osswald and G. Menges, *Materials Science of Polymers for Engineers* (Hanser, München, 2002).